Friction **11**(10): 1804–1814 (2023)
https://doi.org/10.1007/s40544-022-0696-4
ISSN 2223-7690
CN 10-1237/TH

RESEARCH ARTICLE

Tribochemical synthesis of functionalized covalent organic frameworks for anti-wear and friction reduction

Xiaozhi ZHANG[1], Qi LU[1], Yaojie YAN[1], Tingting ZHANG[1], Shujuan LIU[1,*], Meirong CAI[2], Qian YE[1,*], Feng ZHOU[2], Weimin LIU[2]

[1] *State Key Laboratory of Solidification Processing, Center of Advanced Lubrication and Seal Materials, School of Materials Science and Engineering, Northwestern Polytechnical University, Xi'an 710072, China*

[2] *State Key Laboratory of Solid Lubrication, Lanzhou Institute of Chemical Physics, Chinese Academy of Sciences, Lanzhou 730000, China*

Received: 10 June 2022 / Revised: 30 July 2022 / Accepted: 14 September 2022

Abstract: Tribochemistry can be defined as a field dealing with the chemical reactions occurring in the friction zone, capable of catalyzing mechanical and physico-chemical changes in the friction contact area, facilitating the formation of tribo-films, which is also an efficient approach to fabricate novel innovative materials. In this paper, we report the successful synthesis of the silicon oil (SO)-functionalized covalent organic frameworks (COFs) prepared via the tribochemical method when subjected to the reciprocating friction; during the friction process, the rich aldehyde-terminated COFs can bond with amino SO via the Schiff base reaction between aldehyde group and amino group to obtain the desired functionalized COFs (SO@COF-LZU1). The tribochemical reaction progress was tracked through *in-situ* monitoring of the friction coefficient and the operating conditions during the entire friction process. Noticeably, the friction coefficient continued to decrease until it finally stabilized as the reaction progressed, which revealed the formation of a protective tribo-film. Herein, an approximate tribochemical model was presented, wherein the reaction mechanism was investigated and analyzed by employing structural analysis techniques like magic angle spinning nuclear magnetic resonance (MAS NMR), transmission electron microscopy (TEM), and X-ray photoelectron spectroscopy (XPS). Furthermore, the tribochemical-induced SO@COF-LZU1 exhibited remarkable tribological performance with a low friction coefficient of 0.1 and 95.5% reduction in wear volume when used as additives of 500SN base oil. The prime focus of our research was on the preparation and functionalization of COF materials via tribochemical reactions, unraveling a new avenue for the rational design and preparation of functional materials.

Keywords: tribochemical reaction; covalent organic frameworks (COFs); silicon oil (SO) functionalization; lubricant additives; tribological properties

1 Introduction

Friction and wear are two perpetual key challenges for almost all machine elements and industrial components, which often result in excessive energy consumption and equipment failure, triggering huge economic losses [1, 2]. From the various strategies proposed for reducing friction and wear of mechanical systems, the selection of base oil and lubricant additives has emerged as two beneficial approaches to improve the lubrication performance of mechanical equipment [3]. By and large, the lubrication behavior of most lubricants is primarily influenced by the properties of nano-additives, friction pairs, and the service conditions involved [4, 5]. In comparison to that of traditional lubricant additives, the strategy of adding

* Corresponding authors: Shujuan LIU, E-mail: liusj@nwpu.edu.cn; Qian YE, E-mail: yeqian213@nwpu.edu.cn

nanoparticles to various lubricating oils has garnered immense interest from researchers owing to their outstanding tribological characteristics, including wear-resistance and friction-reduction, as well as their environmental sustainability [6, 7].

The term "tribochemistry" is used to describe the chemical reactions occurring between the lubricants and friction pairs during the friction process undergoing extreme frictional conditions such as high frequencies and loads, which are often triggered by virtue of the applied force and the active inorganic/organic molecules added to the lubricants, hence giving rise to the intermediate layers denoted as tribo-films [8–10]. The tribochemical reactions of nano-additives are absolutely vital in the friction process, as they facilitate the formation of protective films, thereby minimizing the direct contact area between the friction pairs [11, 12]. Evidently, the chemical mechanism of tribo-film formation is regulated by the tribochemical reactions [13], while the chemical composition and stereochemistry of the nano-additives on the sliding interface can affect the reaction rate of their tribochemistry [14]. Nonetheless, it is difficult to depict the exact mechanism of the tribochemical reactions taking place due to the complexity of the friction environment. The formation of tribo-films via tribochemical reactions on the wear surfaces can be analyzed after undergoing tribological tests rather than conducting a real-time observation of the ongoing reactions, whereas the postprocessing analysis of the tribo-films is insufficient to explain the actual reactions and formation process of the films [15]. Thus, computer simulation methods, such as molecular dynamics simulation and first-principle calculation, are used to comprehensively elucidate the tribochemical processes at the atomic level [16].

In recent times, the studies on tribochemical reactions predominantly focused on the aspects of friction-reduction and anti-wear mechanisms of lubricants as well as the angle of reactive molecular dynamics simulation [16–18], but very few studies have been conducted on the tribochemical reactions for synthesis or functionalization, with friction coefficient curves tracking the reaction progress. In fact, tribochemical reactions can be deemed as an efficient way of preparing conducive novel materials by means of frictional heat, triboplasma, and triboemission [19, 20], which are different from the traditional parameters of chemical reactions such as heating, photon irradiation, or electrical bias [21]. It is generally acknowledged that tribochemical reactions can take place even without adequate frictional heat and abrasive dust, while the energy inputted by the external mechanical force is supposed to directly act on the reaction system, thereby inducing distortion and dissociation of the organic molecules [22]. For example, Nevshupa et al. [23] observed the tribochemical dehydriding of magnesium hydride in vacuum, which manifested a much higher hydrogen production rate than thermal decomposition. Ramirez et al. [24] reported the tribochemical conversion of methane to graphene and other carbon nanostructures on the sliding Cu/Ni-based coatings under radial load, where the fabrication of carbon film via tribochemical reaction drastically reduced the friction coefficients.

Two-dimensional (2D) materials such as graphene, hexagonal boron nitride, and transition metal dichalcogenides with nanoscale layered structures, low densities, and high specific surface areas possess high thermal stability and high mechanical strengths at the same time, and have shown huge potential in the field of solid lubrication and lubricant additives [25, 26]. When subjected to the radial load and shear force on the friction interface, the easy shearing nanolayers of 2D materials construct a sliding system with rubbing contact and contribute to the anti-friction effect [27]. As lubricant additives, they are easy to enter the contact area and absorb to the substrate due to their high surface energy and van der Waals forces, hence playing a self-healing role remarkably [28]. As a kind of typical 2D nanomaterial, covalent organic frameworks (COFs) with flexible structures, designable functional groups, and abundant active sites have arisen as excellent candidates for tribological applications, and have evoked immense interest among material science researchers to explore the possibility of 2D COFs as lubricant nano-additives [29]. Wen et al. [30] prepared alkyl carboxylic acid-functionalized triazine-based 2D COF nanoplatelets as lubricant additives, which demonstrated impeccable tribological performance attributable to the multilayer tribo-film achieved via 2D COF layers and oxide layers. Zhang

et al. [31] prepared dialkyl dithiophosphate (DDP)-functionalized 2D COFs via the ultraviolet (UV)-induced thiol–ene "click" reaction, and the as-obtained functionalized 2D COFs exhibited remarkable anti-wear and friction reduction performance as oil-based lubricant additives.

Herein, we successfully prepared silicon oil (SO)-functionalized COFs (SO@COF-LZU1) through the tribochemical method under reciprocating friction. The rich aldehyde-terminated COF-LZU1 bonded with amino SO via the Schiff base reaction with aldehyde and amino groups during the friction process. The operating conditions and the friction coefficients were *in-situ* monitored during the entire friction process in order to efficiently track the tribochemical reaction, and it was found that the friction coefficient curves continued to decrease in the run-in period until they stabilized, which can be attributed to the tribochemical reaction progress and the formation of protective tribo-film. Additionally, the as-prepared SO@COF-LZU1 demonstrated remarkable tribological performance as additives for lubricant base oil 500SN. The lubrication mechanism is discussed in detail in the Section 3.

2 Experimental

2.1 Materials

1,3,5-triformylbenzene (TFB), 1,4-diaminobenzene (PDA), and 1,4-dioxane (99.7%, extra dry) were purchased from Energy Chemical. Acetic acid (analytical reagent (AR), 99.8%), N,N'-dimethylformamide (AR, 99.5%), acetone (AR, 99.5%), tetrahydrofuran (AR, 99.0%), and dichloromethane (AR, 99.5%) were obtained from Sinopharm Chemical Reagent Co. Ltd. Amino SO was purchased from Wacker Chemie AG (WR301CN, commercial product). Phenyl SO was acquired from Shanghai Guiyou New Material Technology Ltd. (255-150, commercial product). Lubricant base oil was obtained from Lanzhou Institute of Chemical Physics, Chinese Academy of Sciences (500 SN).

2.2 Preparation of COF-LZU1

The synthesis method of COF-LZU1 was followed in Ref. [32]. 50 mg (0.315 mmol) of TFB, 48 mg (0.3 mmol) of PDA, and 3 mL of 1,4-dioxane were added into an ampule tube. After sonicating the mixture for a few minutes, 0.6 mL of 3 mol/L acetic acid was mixed into the formed clear solution. The tube was rapidly frozen in liquid nitrogen, followed by being vacuumed for 15 min, and then thawed. The procedure of freeze–vacuum–thaw was repeated for 3 times. Subsequently, the tube was sealed by flame, warmed to room temperature, and then left at 120 °C for 72 h. After cooling down, the product was filtered and washed with N,N'-dimethylformamide, acetone, and tetrahydrofuran, and purified by Soxhlet extraction in tetrahydrofuran for 48 h until the solution was clear. Finally, the yellow powders were vacuum dried for 12 h at 80 °C (83.4 mg, 97.9%). Since the ratio of aldehyde group and amino group involved in the reaction is 1.05:1, the as-synthesized COF-LZU1 is aldehyde-terminated.

2.3 Preparation of SO-functionalized COFs (SO@COF-LZU1)

The as-prepared aldehyde-terminated COF-LZU1 was mixed into amino SO WR301CN in a series of different proportions. The mixture was added into the gap between the ball and the disk of tribometer (SRV-V), and then the oscillating reciprocating mode was maintained for 1 h to facilitate the Schiff base reaction. Finally, the product was collected meticulously and filtered under vacuum, washed with dichloromethane to scour off surplus SO, and then dried at 40 °C to obtain SO@COF-LZU1.

2.4 Characterization

The Fourier transform infrared (FT-IR) spectra of the obtained COFs were recorded by an infrared spectrometer (Tensor II, Bruker). The solid-state ^{13}C nuclear magnetic resonance (NMR) data were collected on a 400 MHz NMR spectrometer (Bruker). The morphologies of the COFs were observed by a field emission scanning electron microscope (FESEM; Gemini 500, Zeiss) and a focused ion beam-SEM (FIB-SEM; Helios G4 CX, FEI). The transmission electron microscopy (TEM) images and energy dispersive spectroscopy (EDS) mappings were obtained on the transmission electron microscopes (Double Cs corrector

and Talos F200X, FEI, respectively). The N_2 adsorption–desorption isotherms were taken at −196 °C on an analyzer (ASAP 2460, Micromeritics). The powder X-ray diffraction (PXRD) patterns were characterized on a powder X-ray diffractometer (Ultimate IV, Rigaku) with a Cu Ka radiation (λ = 0.154 nm). The thermogravimetric (TGA) analysis was conducted using a simultaneous thermal analyzer (STA 449F3, NETZSCH). The surface elemental species and chemical states were examined through an X-ray photoelectron spectrometer (5000 VersaProbe III, PHI). A zeta potential analyzer (Zetasizer Nano, Malvern) was employed to detect the surface charge. The water contact angles (CAs) were measured by an optical CA meter (DSA).

The tribochemical reaction and the tests of tribochemical properties were conducted on the SRV-V tribometer by the optimal, utilizing the oscillating reciprocation of the ball-on-disc mode. The upper ball was made of American Iron and Steel Institute (AISI) 52100 steel ($\varnothing$ = 10 mm, 60±2 HRC, and R_a = 0.02 μm), while the lower disk was the same steel ($\varnothing$ = 24 mm × 7.9 mm, 62±2 HRC, and R_a = 0.017 μm). The volume losses and morphologies of the worn surfaces on the steel disk were monitored via a three-dimensional (3D) surface profiler (NPFLEX, Bruker).

3 Results and discussion

The tribochemical synthesis of SO@COF-LZU1 was completed using the SRV-V tribometer, and the set-up conditions were 30 °C, 25 N (9.139×10^8 Pa) with the reciprocating frequency of 25 Hz and the stroke of 1 mm. The functional groups and chemical structures of the commercial amino SO WR301CN are determined by the FT-IR and NMR spectra, respectively (Fig. S1 in the Electronic Supplementary Material (ESM)). Figure 1(a) displays the structures of COF-LZU1 and SO@COF-LZU1, while the tribochemical synthesis mechanism of SO@COF-LZU1 is illustrated in Fig. 2. Subjected to severe conditions of high oscillation frequency, heavy load, shear force, and friction heat, aldehyde-terminated COF-LZU1 and amino SO merge with each other through the Schiff base reaction. To track the progress of the tribochemical reaction, friction coefficient curves of COF-LZU1-based amino SO with different concentrations were recorded for 1 h (Fig. S2(a) in the ESM). It can be seen that the friction coefficient keep decreasing with the fluctuations of the system, which signifies the progress of the Schiff base reaction. In particular, amino SO WR301CN+0.025 wt% COF-LZU1 exhibits an ultra-low and stable friction coefficient of 0.026 after a run-in period of about 30 min (Fig. 1(b)), while the wear volume and scar morphology of 0.025 wt% present similar superiority (Figs. S2(b) and S2(c) in the ESM). Because the adsorption effect of the iron substrate acts on the siloxane chains, SO@COF-LZU1 gets deposited on the surface of the friction pairs to build a protective film and thereby to contribute to

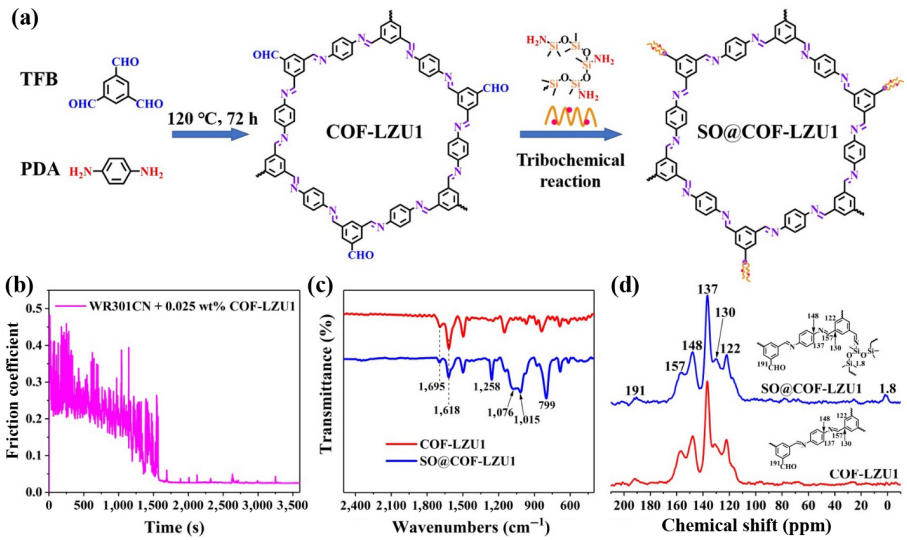

Fig. 1 (a) Synthesis process of COF-LZU1 and SO@COF-LZU1; (b) friction coefficient curve of WR301CN+0.025 wt% COF-LZU1 during the tribochemical reaction; and (c, d) FT-IR and ^{13}C NMR spectra of COF-LZU1 and SO@COF-LZU1, respectively.

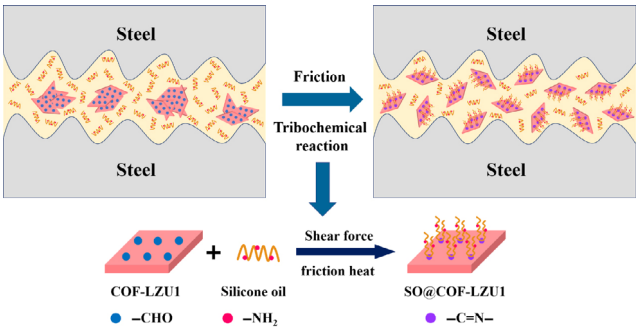

Fig. 2 Tribochemical synthesis process of SO@COF-LZU1.

the ultra-low friction coefficient. The SEM images of the worn surfaces depict a similar contrast (Fig. S3 in the ESM), in which the WR301CN-based worn surface displays deep scratches and apparent plastic deformation, while the 0.025 wt% COF-LZU1-based worn surface appears leveled with shallower grooves. Besides, the X-ray photoelectron spectroscopy (XPS) curve-fitted spectra of the WR301CN-based worn surface are shown in Fig. S4 in the ESM, demonstrating the uniform tribo-film covering the worn surface.

To verify the occurrence of the friction-promoted Schiff base reaction, a series of characterization was carried out in detail. Firstly, the FT-IR spectra were recorded to examine the participating functional groups. The FT-IR spectrum of COF-LZU1 represents visible C=N stretching vibration at 1,618 cm^{-1} and a weakened absorption peak of C=O at 1,695 cm^{-1}, which are indicative of the aldehyde-terminated COF-LZU1 being successfully synthesized (Fig. S5 in the ESM) [33]. Moreover, since the dosage of TFB is slightly in excess in the solvothermal reaction, there is almost no N–H signal presented in the FT-IR spectrum of aldehyde-terminated COF-LZU1, which behaves in conformity with our expectation. As shown in Fig. 1(c), SO@COF-LZU1 exhibits typical Si–O–Si peaks at 1,015 and 1,076 cm^{-1} and Si–CH_3 peaks at 799 and 1,258 cm^{-1}, implying the successful modification of SO onto the COF-LZU1 layers [34].

The solid-state ^{13}C NMR spectra were measured to determine the molecular structures of COF-LZU1 and SO@COF-LZU1. As shown in Fig. 1(d), the ^{13}C NMR peak at 157 ppm can be attributed to the carbon atom of C=N bond, which is produced via the reaction of amino and aldehyde group. The peaks located at 122, 130, 137, and 148 ppm are ascribed to carbon atoms located in the respective positions on the benzene rings, while the peak at 191 ppm is the signal of terminal aldehyde carbon atom [32]. In particular, SO@COF-LZU1 presents a very distinct peak at 1.8 ppm, corresponding to the methyl carbon atom, signifying the presence of the siloxane chains.

The morphologies of the samples before and after undergoing the tribochemical reaction were characterized by means of the SEM and TEM images. Figure S6 in the ESM displays the SEM images of COF-LZU1 and SO@COF-LZU1. As shown in Fig. S6(a) in the ESM, the obtained COF-LZU1 has uniform particles, which is consistent with Ref. [32], while the SO@COF-LZU1 particles show similar morphology but are smaller in size (Fig. S6(b) in the ESM). This is due to that the particles were broken under the action of radial pressure and shear force during the tribochemical reaction process. The high-resolution TEM images and EDS mappings of the COFs with and without the modification of amino SO are enumerated in Fig. 3. The layered stacking structure of COF-LZU1 is clearly shown in Fig. 3(a) and Fig. S7 in the ESM, which appears identical with Ref. [32]. Comparatively, the siloxane-grafted SO@COF-LZU1 represents much smaller layers than COF-LZU1 (Fig. 3(b)), and a heterogeneous layer could be seen along the boundary of the layers (Fig. 3(c)). The EDS mappings reveal the enrichment of silicon and oxygen near the edge of the grafted layers (Figs. 3(d)–3(f)), while carbon and oxygen are evenly distributed throughout the layers (Fig. S8 in the ESM). This serves as the imperative corroboration, reflecting the successful grafting of SO via the tribochemical reaction.

The N_2 adsorption–desorption test was conducted to compare the pore structures of COF-LZU1 and SO@COF-LZU1. As shown in Figs. 4(a) and 4(b), COF-LZU1 exhibits a high N_2 adsorption ability at $P/P_0 < 0.1$ and contains plentiful micropores with a width of 1.2 nm. The Brunauer–Emmett–Teller (BET) surface area of COF-LZU1 is as high as 557.3 $m^2 \cdot g^{-1}$, while SO@COF-LZU1 displays a specific surface area of only 10.8 $m^2 \cdot g^{-1}$. Especially, SO@COF-LZU1 contains only a few pores larger than 7 nm and no micropores at all. This also serves as valuable evidence of the occurrence of the tribochemical reaction, suggesting

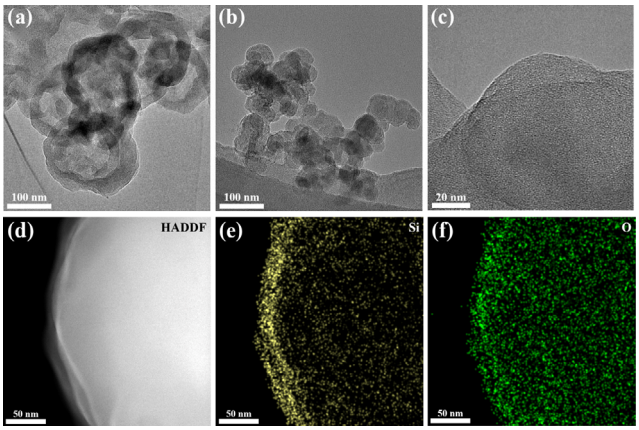

Fig. 3 TEM images of (a) COF-LZU1 and (b, c) SO@COF-LZU1; (d) high-angle annular dark-field (HAADF) image; and (e, f) Si and O elemental mappings of SO@COF-LZU1, respectively.

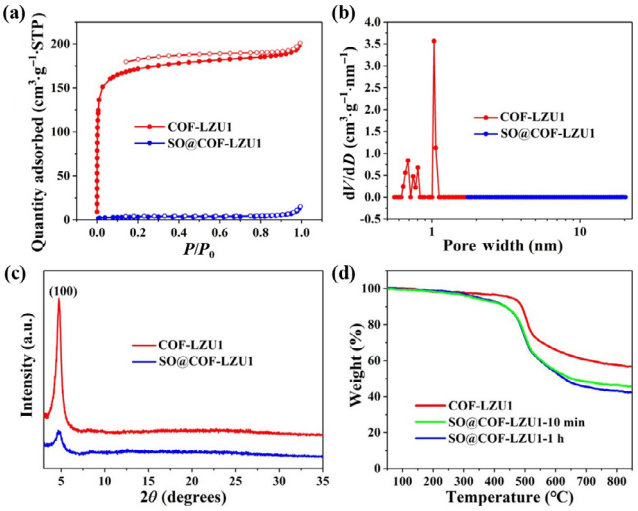

Fig. 4 (a) N_2 adsorption/desorption isotherms and (b) corresponding pore size distributions using the nonlocal density functional theory (NLDFT) model of COF-LZU1 and SO@COF-LZU1; (c) PXRD patterns of COF-LZU1 and SO@COF-LZU1; and (d) TGA curves of the typical samples.

that the pore structures of the COFs are blocked by the siloxane chains. Besides, the PXRD patterns confirm that the SO@COF-LZU1 possesses inferior crystallinity, and its structure is damaged to a certain extent, since its (100) diffraction peak is evidently weaker than that of COF-LZU1 (Fig. 4(c)).

The TGA analysis was carried out from room temperature to 850 °C to evaluate the progress of the tribochemical reaction over an extended period. As shown in Fig. 4(d), COF-LZU1 retains 56.8% of its weight after being calcined to 850 °C, while SO@COF-LZU1, after reciprocating for 10 min and 1 h, retains 45.7% and 42.4% of their weights, respectively. From the above data, it can be calculated that 11.1% of the SO weight is grafted onto COF-LZU1 after undergoing the Schiff base reaction for about 10 min and 14.4% after 1 h, which significantly points that the quantity of the siloxane chains grafting onto the COF-LZU1 tends to increase as the reaction progresses. This also appears consistent with the run-in period data analyzed above.

The XPS spectra were obtained to detect the surface chemical states of COF-LZU1 and SO@COF-LZU1. The full spectrum of SO@COF-LZU1 in Fig. 5(a) denotes the appearance of Si element post undergoing the tribochemical Schiff base reaction, and the peaks at 101.8 and 102.4 eV correspond to Si $2p_{3/2}$ and Si $2p_{1/2}$ electronic states, respectively (Fig. S9 in the ESM). The C 1s spectra of SO@COF-LZU1 are recorded in Fig. 5(b), in which C–Si peak is located at 284.3 eV [35]. Simultaneously, there occurs C–C/C=C signal with the binding energy at 284.8 eV and C–N signal at 285.7 eV [36]. The peak at 288.8 eV is attributed to C=N bond generated by the Schiff base reaction and C=O of unreacted aldehyde group [37]. As shown in Fig. 5(c), the spectra of N 1s display visible peaks at 397.8, 398.8, and 400.2 eV, which are attributed to N–Si, N–H, and C=N–C electronic states, respectively [38, 39]. Besides, the C=N–C peak corresponds significantly well with the peak of C 1s at 288.8 eV.

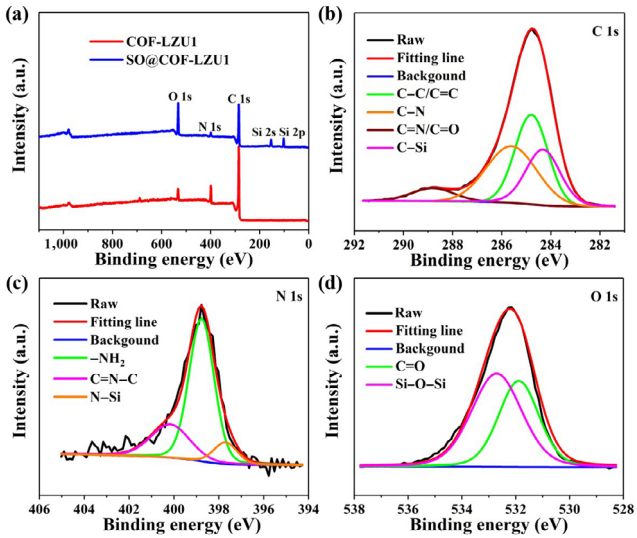

Fig. 5 (a) XPS survey spectra of COF-LZU1 and SO@COF-LZU1; (b, c, and d) curve-fitted XPS spectra of C 1s, N 1s, and O 1s of SO@COF-LZU1, respectively.

Furthermore, the O 1s spectra can be divided into C=O at 531.9 eV and Si–O–Si at 532.7 eV assigned to siloxane chains (Fig. 5(d)) [39, 40]. These XPS results validate that the SO@COF-LZU1 was successfully synthesized via the tribochemical reaction, in terms of the surface chemical state.

Physical properties of COF-LZU1 and SO@COF-LZU1 were also examined. As shown in Fig. S10 in the ESM, the zeta potential of COF-LZU1 in methanol is −48.7 mV, while the amino SO WR301CN possesses an extreme positive surface charge of +94 mV. As a product of the above two, SO@COF-LZU1 exhibits a zeta potential of +44.5 mV, which lies in between those of WR301CN and COF-LZU1, implying that the modification of SO changes the surface potential of COF-LZU1. From the water CAs of the two samples, an analogous conclusion could be drawn. As shown in Fig. S11 in the ESM, the CA of crystalline polymer COF-LZU1 is 66.0°, while SO@COF-LZU1 represents a super hydrophobic property (CA = 157.9°). Noticeably, the arrangement of the siloxane chains changes the interface condition of the COFs. Based on the above analysis including the friction coefficient curves tracking the tribochemical process, observation of the worn surfaces, and a series of characterizations of the as-obtained SO@COF-LZU1, the pragmatic tribochemical model are finally proposed. High pressures and high reciprocating frequencies generate quantity of heat in a small contact area, hence the elevated temperature as well as the mechanical forces extend a synergistic effect to stimulate the Schiff base reaction on the sliding interface between the lubricants and the friction pair materials. Consequently, the SO-functionalized COFs were successfully synthesized together with the formation of a robust protective film on the interface of the friction pairs, resulting in an ultra-low friction coefficient.

Subsequently, the tribological properties of COF-LZU1 and SO@COF-LZU1 as additives in 500SN lubricant base oil were measured on the SRV-V tribometer. The friction coefficient curves were recorded under the condition of 50 °C, 150 N (1.661×10^9 Pa), and 25 Hz with the stroke of 1 mm. The optimal content of 0.025 wt% was determined in advance (Fig. S12 in the ESM), followed by the measurement of the tribological performances of the samples at the certain content. As shown in Fig. 6(a), 500SN base oil exhibits a constantly high friction coefficient of about 0.18 after reciprocating for 300 s, indicating a seizure failure of oil lubrication. Likewise, 500SN+0.025 wt% COF-LZU1 fails after 900 s. As for 500SN+0.025 wt% SO@COF-LZU1, the friction coefficient becomes stable at 0.1, representing an excellent friction reduction behavior. Figure 6(b) displays the wear volumes of the lower disks lubricated by 500SN with the typical samples added. The wear volumes of 500SN and 500SN+0.025 wt% COF-LZU1 are found to be 1.47×10^5 and 1.39×10^5 μm^3, respectively, while the value of 500SN containing 0.025 wt% SO@COF-LZU1 is as low as 6.6×10^3 μm^3, which suffers a 95.5% reduction in comparison to that of pure 500SN. The 3D contour images of the worn surfaces are shown in Fig. S13 in the ESM. All these measurements demonstrate that SO@COF-LZU1 possesses outstanding anti-friction and anti-wear properties when dispersed to 500SN lubricant base oil.

Furthermore, the XPS spectra was conducted to check the surface chemical states of the tribo-film on the wear scar lubricated by 500SN+SO@COF-LZU1. As shown in Fig. 6(c), the C 1s spectra present peaks at 284.7, 285.8, and 288.5 eV, attributable to the C–C, C–O, and C=O bonds, respectively [41], revealing that the tribochemical reaction took place among air, oil, and SO@COF-LZU1. The O 1s spectra are recorded in Fig. 6(d), from which C–O at 531.8 eV can be decomposed, coinciding with the C 1s spectra. Moreover, the peaks located at 529.8, 530.6, and 532.6 eV correspond to Fe_2O_3, $FeCO_3$, and Si–O bonds, respectively [40, 41], signifying that the lower steel disk joins the reaction during the friction process. The Si 2p spectra shown in Fig. 6(e) can be deconvolved into elemental Si peak (99.3 eV), Fe_2SiO_4 peak (101.8 eV), and silicon oxide SiO_x peak (102.6 eV) [42]. As for Fe 2p spectra (Fig. 6(f)), they contain peaks located at 709.5, 712.3, 719.3, and 725.0 eV, ascribed to FeO, Fe_2O_3, FeO(OH), and Fe $2p_{1/2}$ signals, respectively [31, 39]. Furthermore, peaks at 711.0 and 715.2 eV are attributed to Fe_2SiO_4 and $FeCO_3$, respectively [39, 42], corresponding well with the Si 2p and C 1s spectra given above. All these analyses corroborate the existence of the protective tribo-film, which was

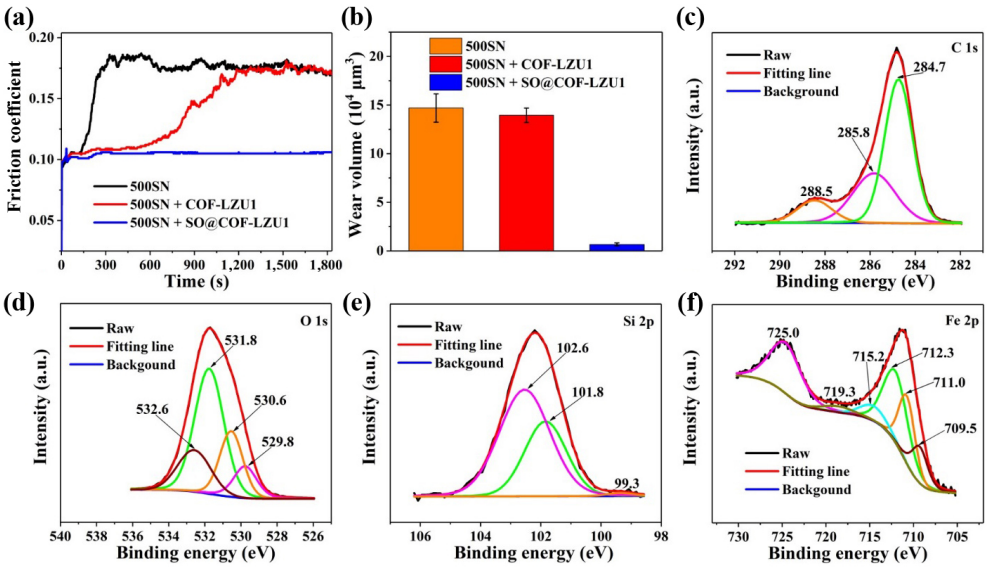

Fig. 6 (a) Friction coefficient curves and (b) wear volume values of typical samples (0.025 wt%); curve-fitted XPS spectra of (c) C 1s, (d) O 1s, (e) Si 2p, and (f) Fe 2p of the worn surface lubricated by 500SN+SO@COF-LZU1.

formed on the worn surface by means of the complex tribochemical reaction while undergoing reciprocating friction.

In addition, the extreme pressure properties of phenyl SO 255-150 with the addition of COF-LZU1 and SO@COF-LZU1 were also measured on the SRV-V tribometer under the condition of 30 °C, 25 Hz, and 1 mm stroke. The load-carrying capacities of 255-150 with varying concentrations of SO@COF-LZU1 are shown in Fig. S14(a) in the ESM, which reveals that the best content of COFs added in 255-150 is 0.01 wt%, while 255-150+0.01 wt% SO@COF-LZU1 bears a load capacity of 32 N. Comparatively, the extreme pressure values of 255-150+0.01 wt% COF-LZU1 and the pure form of 255-150 are both 14 N (Fig. S14(b) in the ESM). Due to the exceptional compatibility between siloxane grafting COFs and phenyl SO, the load-carrying ability of 255-150 is naturally promoted by the microscale addition of SO@COF-LZU1.

Considering the outstanding tribological properties of SO@COF-LZU1, the corresponding lubrication mechanism is depicted in Fig. 7 in detail. Firstly, due to the high surface energy of the COFs and the grafting electron-rich SO chains, SO@COF-LZU1 is easy to enter the contact area and absorb to the iron substrate of the friction pairs. Hence, the nanoscale additives can fill the pits caused by wear and repair the worn surface, playing a remarkable self-healing role [43]. As the oscillation mode reciprocating, tribochemical reaction is induced by the synergetic effect of radial load, shear force, and friction heat, which take place among the iron substrate, base oil, absorbed SO@COF-LZU1, and air. Consequently, the robust tribo-film primarily comprising of Fe and Si oxides is built on the basis of the adsorption film, protecting the friction pairs from further wear. Furthermore, the 2D-functionalized COFs are subjected to the radial load and shear force in the contact area, and hence their easy shearing nanolayers construct a sliding system with rubbing contact and contribute to the anti-friction effect [27]. Besides, on the friction interface, 2D COF nanolayers can be rolled up to nano-rolls, and this kind of structure converts sliding

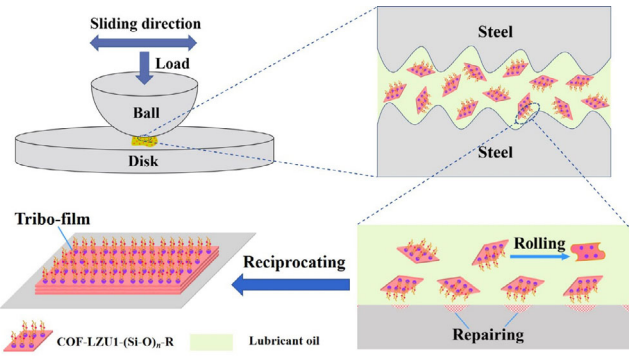

Fig. 7 Lubrication mechanism of SO@COF-LZU1 as lubricant oil additives.

friction into rolling friction and reduces the friction coefficient, which is denoted as rolling effect [44]. In general, it is the tough protective tribo-film that plays the primary role of anti-wear, and the tribo-film effect synergizes with the easy shearing COFs and their rolling effect to reduce friction dramatically.

4 Conclusions

In summary, the desired functionalized COFs SO@COF-LZU1 were successfully synthesized via tribochemical means, where the rich aldehyde-terminated COFs can bond with amino SO via the Schiff base reaction under the synergistic action of the mechanical force and friction heat to produce SO-functionalized COFs. During the friction process, the friction coefficient showed a constant reduction until it stabilized as the tribochemical reaction progressed, which corresponded well with the formation of the protective tribo-film. In particular, the friction coefficient curve of amino SO WR301CN+0.025 wt% COF-LZU1 continued to decline and finally stabilized at an ultra-low value of 0.026, signifying the fabrication process of the tribo-film due to the occurrence of the tribochemical reaction. The tribochemical model was formulated via a series of characterization of the as-prepared SO@COF-LZU1, which also exhibited exceptional tribological properties as additives in 500SN lubricant base oil, with a low friction coefficient of 0.1 and the 95.5% reduction of the wear volume.

Acknowledgements

This work was financially supported by the National Key R&D Program of China (2018YFB0703802), the National Natural Science Foundation of China (U21A2046), and the Fundamental Research Funds for the Central Universities.

Declaration of competing interest

The authors have no competing interests to declare that are relevant to the content of this article. The authors Feng ZHOU and Weimin LIU are the Editorial Board Members of this journal.

Electronic Supplementary Material: Supplementary material is available in the online version of this article at https://doi.org/10.1007/s40544-022-0696-4.

References

[1] Zhai W Z, Bai L C, Zhou R H, Fan X L, Kang G Z, Liu Y, Zhou K. Recent progress on wear-resistant materials: Designs, properties, and applications. *Adv Sci* **8**(11): e2003739 (2021)

[2] Han T Y, Zhang S W, Zhang C H. Unlocking the secrets behind liquid superlubricity: A state-of-the-art review on phenomena and mechanisms. *Friction* **10**(8): 1137–1165 (2022)

[3] Yue W, Sun X J, Wang C B, Fu Z Q, Liu Y D, Liu J J. A comparative study on the tribological behaviors of nitrided and sulfur-nitrided 35CrMo steel lubricated in PAO base oil with MoDTC additive. *Tribol Int* **44**(12): 2029–2034 (2011)

[4] Dai W, Kheireddin B, Gao H, Liang H. Roles of nanoparticles in oil lubrication. *Tribol Int* **102**: 88–98 (2016)

[5] Tang H, Sun J L, He J Q, Wu P. Research progress of interface conditions and tribological reactions: A review. *J Ind Eng Chem* **94**: 105–121 (2021)

[6] Wang Y X, Zhang T T, Qiu Y Q, Guo R S, Xu F, Liu S J, Ye Q, Zhou F. Nitrogen-doped porous carbon nanospheres derived from hyper-crosslinked polystyrene as lubricant additives for friction and wear reduction. *Tribol Int* **169**: 107458 (2022)

[7] Zhai W Z, Srikanth N, Kong L B, Zhou K. Carbon nanomaterials in tribology. *Carbon* **119**: 150–171 (2017)

[8] Hsu S M, Zhang J, Yin Z F. The nature and origin of tribochemistry. *Tribol Lett* **13**(2): 131–139 (2002)

[9] Lu Q, Zhang T T, He B L, Xu F, Liu S J, Ye Q, Zhou F. Enhanced lubricity and anti-wear performance of zwitterionic polymer-modified N-enriched porous carbon nanosheets as water-based lubricant additive. *Tribol Int* **167**: 107421 (2022)

[10] Rana R, Bavisotto R, Hou K M, Tysoe W T. Surface chemistry at the solid–solid interface: Mechanically induced reaction pathways of C_8 carboxylic acid monolayers on copper. *Phys Chem Chem Phys* **23**(33): 17803–17812 (2021)

[11] Spikes H. Friction modifier additives. *Tribol Lett* **60**(1): 5 (2015)

[12] Zhang J, Spikes H. On the mechanism of ZDDP antiwear film formation. *Tribol Lett* **63**(2): 24 (2016)

[13] Zhang J, Ewen J P, Ueda M, Wong J S S, Spikes H A. Mechanochemistry of zinc dialkyldithiophosphate on steel surfaces under elastohydrodynamic lubrication conditions. *ACS Appl Mater Inter* **12**(5): 6662–6676 (2020)

[14] Rana R, Bavisotto R, Hou K M, Hopper N, Tysoe W T. Influence of the nature and orientation of the terminal group on the tribochemical reaction rates of carboxylic acid monolayers on copper. *Tribol Lett* **70**(5): 5 (2022)

[15] Carlton H, Huitink D, Liang H. Tribochemistry as an alternative synthesis pathway. *Lubricants* **8**(9): 87 (2020)

[16] Ta H T T, Tran N V, Tieu A K, Zhu H T, Yu H B, Ta T D. Computational tribochemistry: A review from classical and quantum mechanics studies. *J Phys Chem C* **125**(31): 16875–16891 (2021)

[17] Dong R, Bao L Y, Yu Q L, Wu Y, Ma Z F, Zhang J Y, Cai M R, Zhou F, Liu W M. Effect of electric potential and chain length on tribological performances of ionic liquids as additives for aqueous systems and molecular dynamics simulations. *ACS Appl Mater Inter* **12**(35): 39910–39919 (2020)

[18] Vakis A I, Yastrebov V A, Scheibert J, Nicola L, Dini D, Minfray C, Almqvist A, Paggi M, Lee S, Limbert J, et al. Modeling and simulation in tribology across scales: An overview. *Tribol Int* **125**: 169–199 (2018)

[19] Yeon J, He X, Martini A, Kim S H. Mechanochemistry at solid surfaces: Polymerization of adsorbed molecules by mechanical shear at tribological interfaces. *ACS Appl Mater Inter* **9**(3): 3142–3148 (2017)

[20] Kajita S, Righi M C. Insights into the tribochemistry of silicon-doped carbon-based films by *ab initio* analysis of water–surface interactions. *Tribol Lett* **61**(2): 17 (2016)

[21] Baláž P, Achimovičová M, Baláž M, Billik P, Cherkezova-Zheleva Z, Criado J M, Delogu F, Dutková E, Gaffet E, Gotor F J, et al. Hallmarks of mechanochemistry: From nanoparticles to technology. *Chem Soc Rev* **42**(18): 7571–7637 (2013)

[22] He X, Barthel A J, Kim S H. Tribochemical synthesis of nano-lubricant films from adsorbed molecules at sliding solid interface: Tribo-polymers from α-pinene, pinane, and n-decane. *Surf Sci* **648**: 352–359 (2016)

[23] Nevshupa R, Ares J R, Fernández J F, del Campo A, Roman E. Tribochemical decomposition of light ionic hydrides at room temperature. *J Phys Chem Lett* **6**(14): 2780–2785 (2015)

[24] Ramirez G, Eryilmaz O L, Fatti G, Righi M C, Wen J G, Erdemir A. Tribochemical conversion of methane to graphene and other carbon nanostructures: Implications for friction and wear. *ACS Appl Nano Mater* **3**(8): 8060–8067 (2020)

[25] Liu L, Zhang Y, Qiao Y J, Tan S C, Feng S F, Ma J, Liu Y H, Luo J B. 2D metal–organic frameworks with square grid structure: A promising new-generation superlubricating material. *Nano Today* **40**: 101262 (2021)

[26] Wang H D, Liu Y H. Superlubricity achieved with two-dimensional nano-additives to liquid lubricants. *Friction* **8**(6): 1007–1024 (2020)

[27] Xiao H P, Liu S H. 2D nanomaterials as lubricant additive: A review. *Mater Design* **135**: 319–332 (2017)

[28] Shi H Y, Lu X C, Liu Y H, Song J, Deng K, Zeng Q D, Wang C. Nanotribological study of supramolecular template networks induced by hydrogen bonds and van der Waals forces. *ACS Nano* **12**(8): 8781–8790 (2018)

[29] Wen P, Zhang C Y, Yang Z G, Dong R, Wang D M, Fan M J, Wang J Q. Triazine-based covalent-organic frameworks: A novel lubricant additive with excellent tribological performances. *Tribol Int* **111**: 57–65 (2017)

[30] Wen P, Lei Y, Yan Q, Han Y, Fan M. Multilayer tribofilm: An unique structure to strengthen interface tribological behaviors. *ACS Appl Mater Inter* **13**(9): 11524–11534 (2021)

[31] Zhang T T, Liu S, Zhang X Z, Gao J D, Yu H, Ye Q, Liu S J, Liu W M. Fabrication of two-dimensional functional covalent organic frameworks via the thiol–ene "click" reaction as lubricant additives for antiwear and friction reduction. *ACS Appl Mater Inter* **13**(30): 36213–36220 (2021)

[32] Ding S Y, Gao J, Wang Q, Zhang Y, Song W G, Su C Y, Wang W. Construction of covalent organic framework for catalysis: Pd/COF-LZU1 in Suzuki–Miyaura coupling reaction. *J Am Chem Soc* **133**(49): 19816–19822 (2011)

[33] Shi Y N, Zhang X F, Liu H T, Han J Y, Yang Z J, Gu L, Tang Z Y. Metalation of catechol-functionalized defective covalent organic frameworks for Lewis acid catalysis. *Small* **16**(24): e2001998 (2020)

[34] Puneetha P, Mallem SPR, Lee YW, Shim J. Strain-controlled flexible graphene/GaN/PDMS sensors based on the piezotronic effect. *ACS Appl Mater Inter* **12**(32): 36660–36669 (2020)

[35] O'Hare L A, Parbhoo B, Leadley S R. Development of a methodology for XPS curve-fitting of the Si 2p core level of siloxane materials. *Surf Interface Anal* **36**(10): 1427–1434 (2004)

[36] Yang S Y, Liu Y, Mao J, Wu Y B, Deng Y L, Qi S C, Zhou Y C, Gong S Q. The antibiofilm and collagen-stabilizing effects of proanthocyanidin as an auxiliary endodontic irrigant. *Int Endod J* **53**(6): 824–833 (2020)

[37] Wen P, Lei Y Z, Li W Q, Fan M J. Two-dimension layered nanomaterial as lubricant additives: Covalent organic frameworks beyond oxide graphene and reduced oxide graphene. *Tribol Int* **143**: 106051 (2020)

[38] Zhao K, Cheng L F, Ye F, Cheng S, Cui X F. Preparation and performance of Si_3N_4 hollow microspheres by the template method and carbothermal reduction nitridation. *ACS Appl Mater Inter* **11**(42): 39054–39061 (2019)

[39] Ye Q, Liu S, Zhang J, Xu F, Zhou F, Liu W M. Superior lubricity and antiwear performances enabled by porous carbon nanospheres with different shell microstructures. *ACS Sustain Chem Eng* **7**(14): 12527–12535 (2019)

[40] Bao C, Xu K Q, Tang C Y, Lau W M, Yin C B, Zhu Y, Mei J, Lee J, Hui D, Nie H Y, et al. Cross-linking the surface of cured polydimethylsiloxane via hyperthermal hydrogen projectile bombardment. *ACS Appl Mater Inter* **7**(16): 8515–8524 (2015)

[41] Ye Q, Liu S, Xu F, Zhang J, Liu S J, Liu W M. Nitrogen–phosphorus codoped carbon nanospheres as lubricant additives for antiwear and friction reduction. *ACS Appl Nano Mater* **3**(6): 5362–5371 (2020)

[42] Zhao J, Wu C, Luo D H, Yan M. Soft magnetic composites based on the Fe elemental, binary and ternary alloy systems fabricated by surface nitridation. *J Magn Magn Mater* **481**: 140–149 (2019)

[43] Guo Y B, Zhou X L, Lee K, Yoon H C, Xu Q, Wang D G. Recent development in friction of 2D materials: From mechanisms to applications. *Nanotechnology* **32**(31): 312002 (2021)

[44] Bai Y Q, Zhang J, Wang Y F, Cao Z Y, An L L, Zhang B, Yu Y L, Zhang J Y, Wang C M. Ball milling of hexagonal boron nitride microflakes in ammonia fluoride solution gives fluorinated nanosheets that serve as effective water-dispersible lubricant additives. *ACS Appl Nano Mater* **2**(5): 3187–3195 (2019)

Xiaozhi ZHANG. He received his B.E. degree at School of Materials Science and Engineering, Northwestern Polytechnical University, China, in 2019. He is currently a doctoral student at Center of Advanced Lubrication and Seal Materials, Northwestern Polytechnical University, China. His research interest is functionalized covalent organic frameworks for lubrication.

Qian YE. He is an associate professor at Northwestern Polytechnical University, China. He received his B.S. degree at Lanzhou University, China, in 2005, and got his Ph.D. degree in organic chemistry at Lanzhou University, China, in 2010. He spent one year (2013–2014) at Université catholique de Louvain, Belgium, as a research associate. His research interests focus on functional nanomaterials, surface modification, lubricant coating, and anti-fouling materials. His work has been published in more than 80 peer-reviewed papers with a current h-index of 30.

Shujuan LIU. She is a full professor at Northwestern Polytechnical University, China. She has gained her Ph.D. degree in 2004 at Lanzhou Institute of Chemical Physics, Chinese Academy of Sciences, China, and spent three years (2005–2008) in Department of Chemistry, University of Cambridge, UK, as a research associate. She has published more than 60 papers and 20 patents; her research interests include the functional nanomaterials, lubricant additive, and antibiofouling coatings.